Materials Transactions, Vol. 47, No. 4 (2006) pp. 1066 to 1070
Special Issue on Platform Science and Technology for Advanced Magnesium Alloys, III

Alloy Development of High Toughness Mg-Gd-Y-Zn-Zr Alloys

Kentaro Yamada[1], Yoshiyuki Okubo[2,*1], Masashi Shiono[2,*1], Hidetsuna Watanabe[2,*2], Shigeharu Kamado[2] and Yo Kojima[2]

[1]*Research Center for Advanced Magnesium Technology, Nagaoka University of Technology, Nagaoka 940-2188, Japan*
[2]*Dept. Mechanical Engineering, Nagaoka University of Technology, Nagaoka 940-2188, Japan*

The effects of zinc addition on microstructure evolution and mechanical properties of Mg-Gd-Y-(-Zr) based alloys are investigated in details using OM, TEM, Vickers hardness tests and tensile tests. Specific line-shaped structure is formed inside of matrix grain in the as-cast specimen. This structure is dissolved after a solution-treatment at 773 K. Instead of it, in the 0.3–1Zn alloy, the 14H LPSO structure is observed at grain boundaries of Mg matrix phases after the solution heat treatment. Metastable β' phase is formed during subsequent aging treatment at 498 K. The 14H LPSO structure is stable and remained even after the aging treatment. These structure and phase coexist at the peak-aged condition in the microstructure. In cast- specimens, 0.2% proof stress and tensile strength slightly decreases with an addition of zinc up to 0.75 mol% and rapidly decreases over 1 mol% zinc addition. On the contrary, in rolled-specimens, addition of 0.3–1 mol% zinc improves mechanical properties in both strength and ductility significantly. It is found that the UTSs reach more than 400 MPa in the 0.3–1Zn alloys. This characteristic effect is considered to be the contribution of LPSO structure and its specific orientation relationship with matrix phase.

(Received November 11, 2005; Accepted March 9, 2006; Published April 15, 2006)

Keywords: *long-period ordered structure, age hardening, precipitation, Magnesium-Rear Earth alloy, high strength*

1. Introduction

In recent years, urgent developments of new light structural materials for an aircraft are strongly desired in terms of reduction of fuel efficiency as well as for an automobile. As one of the effective possible applications to the structural parts of an aircraft, high strength Mg-RE (Rare Earth element) based alloys have become attractive for the recent desires over the world. Mg-RE alloys have been well known as typical age-hardenable alloys,[1–7] and it is reported that simultaneous additions of gadolinium and yttrium bring about high strength at high temperature[8,9] and good corrosion resistance[10,11] in recent years. Furthermore, on the one hand, Kawamura *et al.* developed rapidly solidified powder metallurgy (P/M) $Mg_{97}Zn_1Y_2$ alloys which have remarkable high strength (above 600 MPa) and rather high ductility.[12] These high mechanical properties are considered to be achieved by contribution of homogeneous nanocrystalline and non-equilibrium phases obtained by rapid solidification process. Subsequent several micro/nanostructure analyses revealed that the novel long-period stacking ordered (LPSO) structures are formed in the processes of rapid solidification and/or subsequent hot-extrusion of the various $Mg_{97}Zn_1RE_2$ alloys.[13–15] And moreover, it has been found that one type of the LPSO structures is formed even in ingot metallurgy (I/M) $Mg_{97}Zn_1RE_2$ based alloys (including Gadolinium containing alloys) by the following studies for the $Mg_{97}Zn_1RE_2$ alloys. Therefore, it is expected to develop new high strength I/M Mg-RE based alloys which consist of the LPSO structure and magnesium matrix grains by addition of zinc to the Mg-RE alloys. However, since the natures of LPSO structure have still not been understood sufficiently, it is necessary to investigate the characteristics of microstructure and its correlation with mechanical properties basically for the zinc-added Mg-RE alloys. In this paper, we will report the effects of different amounts of zinc addition on microstructure evolution and mechanical properties of I/M Mg-Gd-Y based alloys and their basic characteristics are summarized.

2. Experimental Procedures

Eight Mg-2Gd-1.2Y-Zn-0.2Zr (mol%) alloys which contain different amounts of zinc ranging from 0.05 to 2 mol% are prepared for the specimen in this study. Chemical compositions of specimens are listed in Table 1. Each alloy is named as shown in the table according to the amounts of zinc addition. Zirconium was added for the purpose of grain refinement. All alloy ingots were obtained by conventional casting under an atmosphere of a mixed gas of CO_2 and SF_6 using electric resistance furnace. 99.99% pure magnesium and binary Mg-Gd master alloy were melted at 1053 K firstly and then 99.9% pure zinc, Mg-Y and Mg-Zr pre-heated at ~573 K were added to the melt. After stirring and killing for about 0.9 ks the melt was poured into a book mold held at 473–573 K. Subsequent heat- and mechanical treatments procedures are shown in Fig. 1 schematically. Two procedures are shown for (a) cast-specimens (indicated by black line) and (b) rolled-specimens (indicated by gray line) in the figure. Solution (Homogenization) treatment was carried out

Table 1 Chemical compositions of specimens. mol% (mass%)

Alloys	Gd	Y	Zn	Zr	Mg
0.05Zn	2.0 (11)	1.2 (3.7)	0.05 (0.12)	0.16 (0.52)	bal.
0.1Zn	2.0 (11)	1.2 (3.9)	0.11 (0.26)	0.17 (0.56)	bal.
0.3Zn	2.0 (11)	1.2 (3.7)	0.30 (0.70)	0.18 (0.59)	bal.
0.5Zn	1.8 (10)	1.2 (3.9)	0.46 (1.1)	0.14 (0.45)	bal.
0.75Zn	1.9 (11)	1.3 (4.0)	0.73 (1.7)	0.15 (0.48)	bal.
1Zn	1.9 (11)	1.3 (4.0)	0.99 (2.3)	0.15 (0.48)	bal.
1.5Zn	2.0 (11)	1.3 (4.0)	1.5 (3.5)	0.19 (0.52)	bal.
2Zn	2.0 (11)	1.2 (3.6)	1.9 (4.4)	0.19 (0.60)	bal.

*1Graduate Student, Nagaoka University of Technology
*2Graduate Student, Nagaoka University of Technology. Present address: Hitachi Metals, Ltd., Mooka 321-4367, Japan

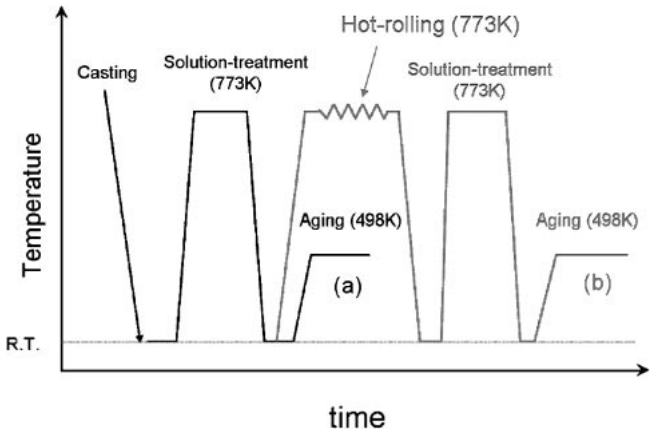

Fig. 1 Schematic illustrations of experimental procedures for the (a) cast- and (b) rolled-specimens.

at 773 K for 36 ks under an argon atmosphere. Then the specimens were quenched into water at room temperature. Hot-rolling was carried out at 773 K for a total reduction ratio of 80% at 10% per pass. Aging heat-treatments were performed at 498 K in a silicone-oil bath. Microstructures of specimens are investigated by OM and TEM. TEM observation was carried out using a JEM 2010 at an accelerating voltage of 200 kV. The samples for TEM were ion milled using the Ion Polishing System. Hardness tests were performed using a Vickers hardness tester, and tensile tests were performed with strain rates of $1 \times 10^{-3}\,s^{-1}$ at room temperature. The tensile axis of sample was parallel to rolling direction for the rolled-specimen.

3. Results and Discussion

3.1 Microstructures and aging characteristics

3.1.1 Cast-specimen

Figure 2 shows optical microstructures of as-cast specimens. By addition of zirconium, magnesium grains are refined and average size of grains is about 50 μm in all alloys. In the 0.05Zn alloy, the microstructure is similar to that of Zn-free alloys. Needle shape precipitates are observed near grain boundaries. These precipitates which are typically observed also in as-cast Mg-Gd and Mg-Y alloys are formed during cooling of ingot after solidification and completely solutionized by subsequent solution (homogenization)-treatment at 773 K. Addition of more than 0.1% zinc causes significant change in microstructure. Fine straight contrasts are uniformly observed at inside of grains in all alloys except the 0.05 alloy. The fine contrast in as-cast specimens has a specific orientation relationship with matrix crystal and this is the one of characteristics of microstructure in Zn-added alloys. In the alloys with zinc addition more than 0.75%, intermetallic compounds are observed at boundaries of magnesium crystals. The detailed identification of this compound is now in progress. The volume fraction of compound increases with an increase of the amount of zinc addition to alloys.

Figure 3 shows optical microstructures of solution-treated (773 K, 36 ks) specimens. Almost all precipitates and straight contrasts which are observed inside of grains in the as-cast specimen disappear after the solution-treatment. This indicates that the structure which corresponds to the straight contrast is unstable at 773 K. Instead of it, another feature of microstructure in Zn-added alloys comes out. In the 0.3–1Zn alloys, distinct straight lamellae are observed at grain boundaries. This lamella also has a specific orientation relationship with matrix crystals as well as the straight contrast observed in the as-cast specimens. However, the size (width) and morphology of them are different from each other and the lamellae are rather stable at 773 K. Therefore, we distinguish the lamellae from the straight contrast. The volume fraction of lamella is highest in the 0.75 alloy. In the 1Zn alloy, unresolved compounds are observed and the volume of lamella decreases. In the 2Zn alloy, almost no lamella is observed and the microstructure consists of the compound and solutionized magnesium grains.

Figure 4 shows isothermal aging curves at 498 K for all cast-specimens. In the alloys with zinc addition less than 0.3%, aging characteristics are almost same as that of Zn free Mg-Gd-Y alloys. However, in the alloys containing zinc less than 0.5%, peak hardness value decreases and aging time to peak hardness becomes longer with an increase of amount of

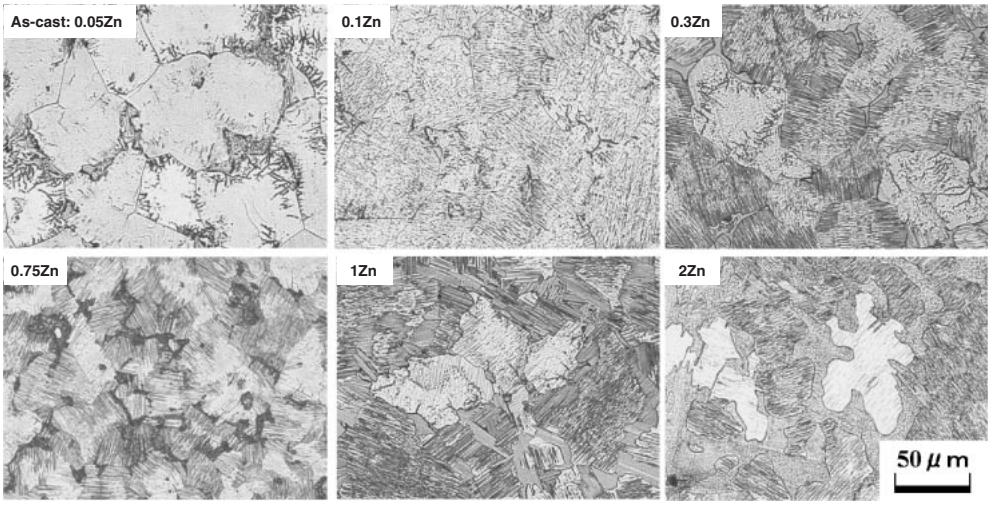

Fig. 2 Optical microstructures of as-cast specimens.

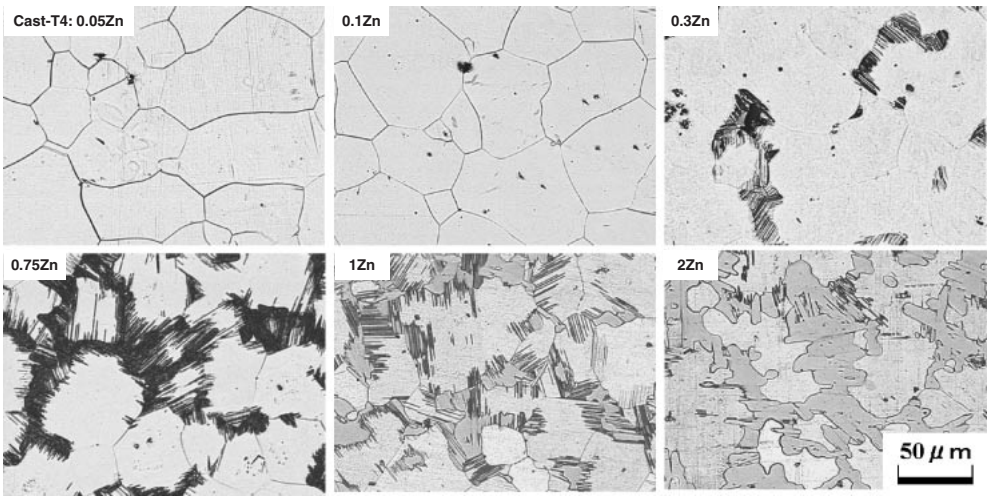

Fig. 3 Optical microstructures of solution-treated (773 K, 36 ks) specimens.

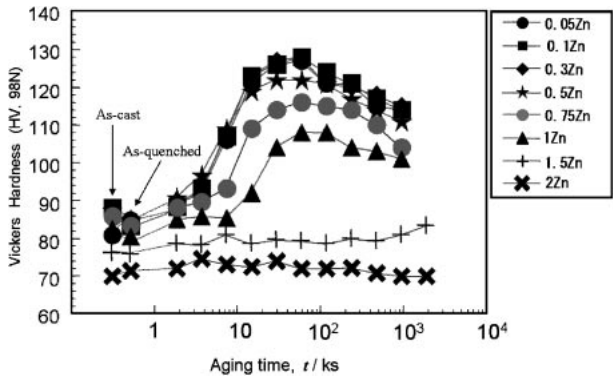

Fig. 4 Isothermal aging curves of cast-specimens at 498 K.

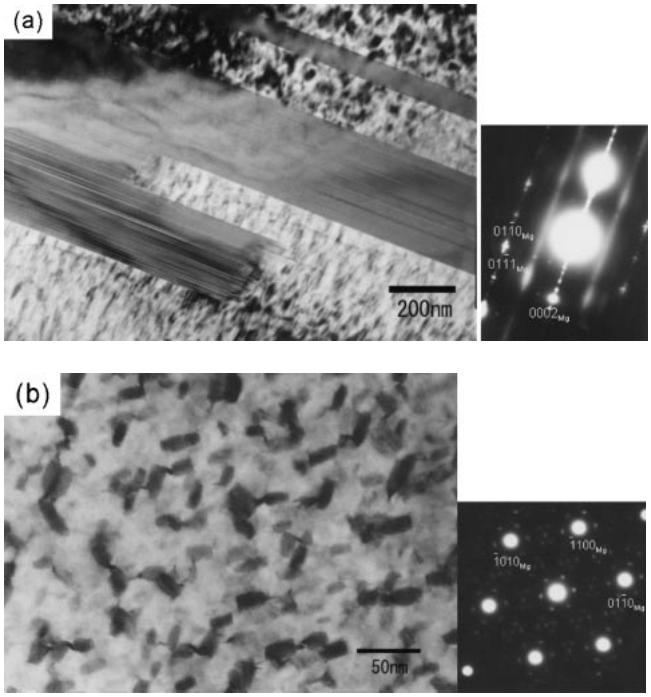

Fig. 5 Bright field images with diffraction patterns for the cast-0.75Zn alloy solution-treated (773 K, 36 ks) then aged (498 K, 36 ks) showing (a) LPSO structures and (b) β' and β_1 phases.

zinc addition. In the alloys containing zinc more than 1.5%, almost no age hardening takes place. This reduction of age hardening response is considered to be due to the remained compound even after the solution treatment as shown in Fig. 3. This suggests that the solubility limit of Gd and Y at 773 K is rapidly decreased by the addition of zinc more than 1%. Significant changes in hardness corresponding to either the formation of straight contrast observed in Fig. 2 or lamella observed in Fig. 3 are not found out.

The TEM microstructures of 0.75Zn alloy at peak aged condition are shown in Fig. 5. Figure 5(a) shows the lamellae and surrounding matrix. Beam direction is parallel to $[2\bar{1}\bar{1}0]_{Mg}$. From the obtained diffraction pattern, the lamella is identified as the 14H LPSO structure.[15] Periodic small diffraction spots are observed at the interval of 1/14 of distance between direct spot and $(0002)_{Mg}$ reflection, and corresponding fringes are observed in the bright field image. Fine strain contrasts are also observed in matrix. These fine contrasts are from metastable β' aging precipitates formed during aging treatment at 498 K. Figure 5(b) shows the picture taken at higher magnification for the β' phase in the same sample. Beam direction is parallel to $[0001]_{Mg}$. Globular precipitates and corresponding diffraction pattern are consistent with those reported in other studies[5,6] and plate-shaped β_1 phases are also observed. This result indicates that zinc addition do not affect the characteristics of aging precipitation sequence in Mg-RE alloys significantly. However, it is noteworthy that there is no precipitate free zone at the interface between the LPSO structures and matrix [Fig. 5(a)]. It is found that the LPSO structure and metastable β' phase coexist in the alloy at the peak aged condition.

3.1.2 Rolled-specimen

Effect of hot-rolling was also investigated. Experimental procedure is shown in Fig. 1(b). Figure 6 shows the optical microstructures of (a) as-rolled specimens and (b) rolled and then solution-treated (773 K, 36 ks) specimens. Since the temperature of hot-rolling is equal to the solution-treatment temperature, no precipitates are observed in the micro-

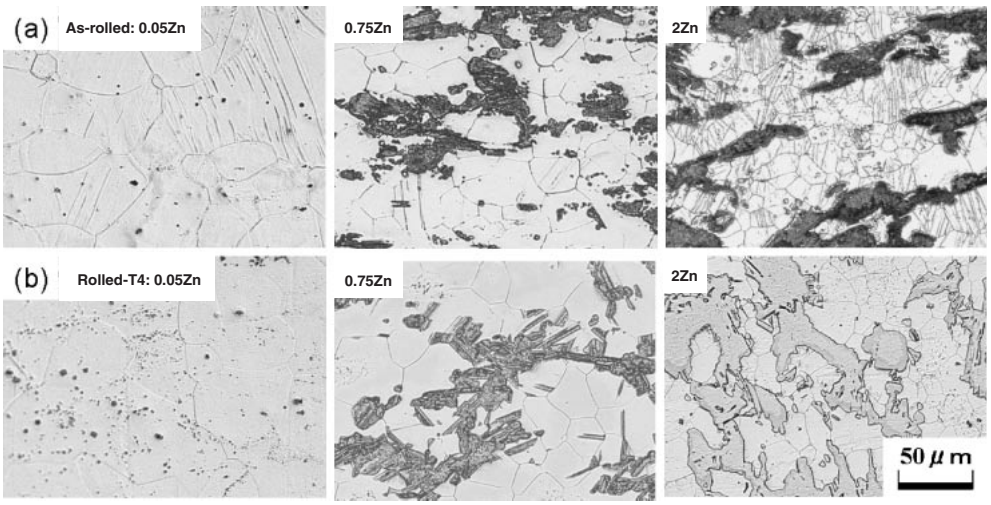

Fig. 6 Optical microstructures of (a) as-rolled specimens and (b) rolled and then solution-treated (773 K, 36 ks) specimens.

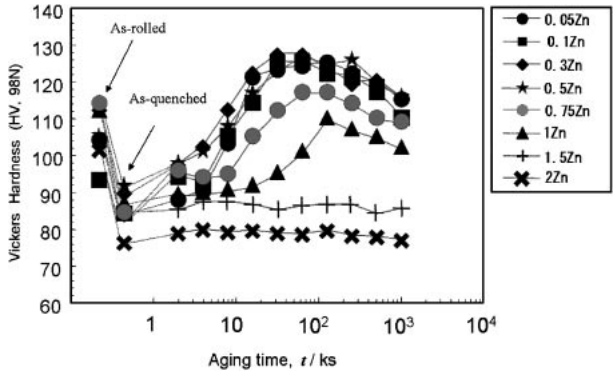

Fig. 7 Isothermal aging curves of rolled-specimens at 498 K.

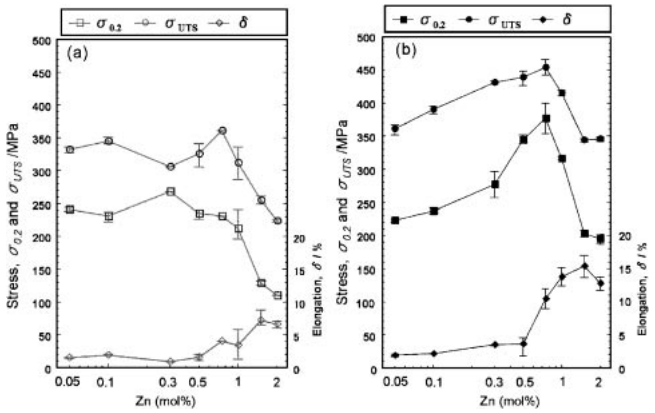

Fig. 8 Tensile properties of (a) cast- and (b) rolled-specimens solution-treated (773 K, 36 ks) then aged (498 K, 36 ks).

structures. Twins are observed in several grains in all specimens, particularly often in the 2Zn alloy. Both the lamellae in the 0.75Zn alloy and compounds in the 2Zn alloy are deformed and distributed ununiformly. Though the grain size in the 0.05Zn alloy is almost same as that before hot-rolling, the grain size in the 0.75Zn and 2Zn alloy are significantly refined. These results suggest that higher strain is induced during the hot-rolling in the higher Zn alloys, and this leads the acceleration of nucleation of recrystallization. Grain growth during solution-treatment is not significant.

Figure 7 shows isothermal aging curves of rolled-specimens. Peak hardness values and hardening characteristics are almost unchanged compared to those of cast-specimen. These results indicate the aging precipitates (such as β' phase) are formed in the rolled-specimens as well as in the cast-specimens.

3.2 Mechanical properties

Tensile properties of cast- and rolled-specimens solution-treated and then aged at 498 K for 36 ks (peak aging condition) are shown in Figs. 8 (a) and (b), respectively.

In cast-specimens, obtained properties are in good agreement with the results of hardness measurements. 0.2% proof stress and tensile strength slightly decreases with an addition of zinc up to 0.75 mol% and rapidly decreases over 1 mol% zinc addition. On the contrary, elongation is increased with an addition of zinc over 0.5 mol%. These decreases of 0.2% proof stress and tensile strength are considered to be due to a decreased number density of β' phase during the aging treatment as a result of the formation of compounds.

On the other hand, in rolled-specimens, obtained properties are characteristic of the multi-phase microstructure which consists of LPSO structure and age-hardened matrix. 0.2% proof stress, elongation and tensile strength, all properties are more improved with an increase of zinc addition up to 0.75 mol%. Particularly, increment of 0.2% proof stress is significant, and moreover, elongation reaches over 10%. It is also found that the UTSs reach more than 400 MPa in the 0.3–1Zn alloys. Though further fundamental investigation seems to be required in order to explain these specific changes, it is considered that the effect of strengthening of LPSO structure should have strong dependency on an orientation relationship between a tensile axis direction and the LPSO structure because the LPSO structure is basically the basal stacking structure of Mg matrix. Therefore, it is necessary to take account of texture formation and to elucidate the correlation between precipitation and recrystallization reaction during the processes in this alloy system for further development as a high strength material.

4. Conclusion

The effects of zinc addition on microstructure evolution and mechanical properties of Mg-Gd-Y-(-Zr) based alloys are investigated and their basic characteristics are summarized as follows:

(1) Specific line-shape structure is formed inside of matrix grain in as-cast specimen. This structure is dissolved by solution-treatment at 773 K.

(2) In the 0.3–1Zn alloy, the 14H LPSO structure is observed at grain boundary of Mg matrix crystals after solution- treatment at 773 K and metastable β' phase is formed during subsequent aging treatment at 498 K. These structure and phase coexist at the peak-aged condition in the microstructure.

(3) In rolled-specimens, addition of 0.3–1 mol% zinc improves mechanical property in both strength and ductility significantly. It is found that the UTSs reach more than 400 MPa. This is considered to be the contribution of LPSO structure.

Acknowledgement

This project was conducted as a part of the project, "Civil Aviation Fundamental Technology Program-Advanced Materials & Process Development for Next-Generation Aircraft Structures" under contract from RIMCOF, founded by the Ministry of Economy, Trade and Industry (METI) of Japan.

REFERENCES

1) S. Kamado, Y. Kojima R. Ninomiya and K. Kubota: *Proc. of 3rd International Magnesium Conf.*, ed. by G. W. Lorimer, (The Institute of Materials, London, 1997) pp. 327–342.
2) Y. Negishi, T. Nishiyama, S. Iwasawa, S. Kamado, Y. Kojima and R. Ninomiya: J. Japan Inst. of Light Metals **44** (1994) 555–561.
3) Y. Negishi, T. Nishiyama, M. Kiryuu, S. Kamado, Y. Kojima and R. Ninomiya: J. Japan Inst. of Light Metals **45** (1995) 57–63.
4) L. Y. Wei, G. L. Dunlop and H. Westengen: J. Mater. Sci. **31** (1996) 387–397.
5) J. F. Nie and B. C. Muddle: Acta Mater. **48** (2000) 1691–1703.
6) P. J. Apps, H. Karimzadeh, J. F. King and G. W. Lorimer: Scripta Mater. **48** (2003) 1023–1028.
7) C. Antion, P. Donnadieu, F. Perrard, A. Deschamps, C. Tassin and A. Pisch: Acta Mater. **51** (2003) 5335–5348.
8) I. A. Annyanwu, S. Kamado and Y. Kojima: Mater. Trans. **42** (2001) 1206–1211.
9) I. A. Annyanwu, S. Kamado and Y. Kojima: Mater. Trans. **42** (2001) 1212–1218.
10) M. Kiryuu, H. Okumura, S. Kamado, Y. Kojima, R. Ninomiya and I. Nakatsugawa: J. Japan Inst. of Light Metals **46** (1996) 39–44.
11) I. Nakatsugawa, S. Kamado, Y. Kojima, R. Ninomiya and K. Kubota: Corros. Rev. **16** (1998) 139–157.
12) Y. Kawamura, K. Hayashi, A. Inoue and T. Masumoto: Mater. Trans. **42** (2001) 1172–1176.
13) E. Abe, Y. Kawamura, K. Hayashi and A. Inoue: Acta Mater. **50** (2002) 3845–3857.
14) K. Amiya, T. Ohsuna and A. Inoue: Mater. Trans. **44** (2003) 2151–2156.
15) T. Itoi, T. Seimiya, Y. Kawamura and M. Hirohashi: Scripta Mater. **51** (2004) 107–111.